

02

## Investigation of dielectric functions of a layer of Ag nanoparticles on silicon using spectro-ellipsometry and spectrophotometry

© V.A. Tolmachev, Yu.A. Zharova, A.A. Ermina, V.O. Bolshakov

Ioffe Institute,  
194021 St. Petersburg, Russia  
e-mail: tva@mail.ioffe.ru

Received August 20, 2021

Revised September 24, 2021

Accepted September 28, 2021

An investigation of the optical characteristics of a layer of Ag nanoparticles deposited from an  $\text{AgNO}_3$  solution on the surface of single-crystal Si is presented. The measurements were carried out using spectroscopic ellipsometry and spectrophotometry at the same tilt angle and sample probe location in a wide spectral range from 200 to 1700 nm. From the obtained experimental data, the parameters of the Drude-Lorentz model and the complex dielectric function were determined, which was compared with the pseudo-dielectric function. Both dependences revealed resonances of a bulk plasmon near the energy  $E = 3.8$  eV, while a localized plasmon was detected in the pseudo-dielectric function at  $E = 1.65$  eV, and in the dielectric function at  $E = 1.84$  eV.

**Keywords:** dielectric function, Drude-Lorentz model, silver nanoparticles, plasmon, pseudo-dielectric function, spectrophotometry, ellipsometry

DOI: 10.21883/EOS.2022.02.53215.2668-21

### 1. Introduction

The optical properties of island films (layers of nanoparticles) of metals are determined by the presence of electrons that can interact with external electromagnetic fields, including excitation of plasmon resonances, which concentrate the received energy into highly localized electric fields [1,2]. The curved surface of the particle has an effective restoring effect on the moving electrons, resulting in field enhancement both inside and in the near field zone outside the particle. Another consequence of surface curvature is that plasmon resonances can be excited by direct light illumination. As a result, the so-called „hot zones“ are created, control of which allows for designing and creating on this basis sensors for chemical and biomedical probing [3]. Also using enhancement of these fields, metal nanoparticles are used to improve efficiency of photovoltaic cells [4] and to design and build photonic metamaterials [5]. Studies of plasmon resonances unite theorists, developers of technologies for obtaining structures and measuring their optical properties. The relevance of such developments was confirmed in the review [6], called the roadmap of plasmonics, which reflects the interest in many of its areas both from the scientific side and from the point of view of application in various fields.

Currently, to obtain layers of silver nanoparticles on substrates, various methods are used, conditionally divided into chemical, using a liquid phase or vapors of silver-containing components (precursors), and physical, using a pure Ag target and exposing it to heating, laser radiation, magnetron excitation, etc. The optical response of an

island-structured Ag film differs from that of a conventional film with plane-parallel interfaces; therefore, the use of effective medium approximations for them is not always successful. For such objects, the Drude-Lorentz (D-L) [7] model is applied, which is used to determine the complex dielectric function  $\varepsilon$  and the parameters that describe it, including the parameters of various oscillators. This function can be determined experimentally in two ways: using transmission and/or reflective spectrophotometry and spectral ellipsometry. Si was used as a substrate, which absorbs light in the visible and ultraviolet (UV) regions of the spectrum, which makes it difficult to measure the optical transmission. In this case, the methods of reflective spectrophotometry [8,9] and spectral ellipsometry [10,11] are used. On the obtained reflection spectra  $R$ , their features are analyzed in the form of maxima and dips both in amplitude and in width.

The aim of this article was to characterize the optical and plasmonic features of Ag nanoparticle layer deposited on a single-crystal Si substrate using spectral ellipsometry and reflective spectrophotometry in the range from UV to near IR at an oblique incidence angle  $\varphi$ . These measurements were carried out at the same angle  $\varphi$  and the same sample location. The measured data were interpreted using the „external medium-substrate“ models with calculation of the pseudodielectric function  $\langle\varepsilon\rangle$  [11] and the „external medium-film-substrate“ model using the D-L formula. As a result of fitting the calculated ellipsometric spectra and the  $R$  spectra to the experimentally measured spectra, the dependences  $\varepsilon$  were determined and compared with  $\langle\varepsilon\rangle$ .

## 2. Method of obtaining Ag nanoparticles on Si surface

As a rule, nanoparticle layer has small effective thickness, and the optical properties of the substrate can contribute to the optical response, which must be taken into account both in calculations and in the interpretation of the experiment. Before Ag nanostructures are deposited on a Si substrate, a layer of SiO<sub>2</sub> is usually formed with much greater thickness than for natural oxide, which is connected either to create an insulating layer for subsequent evaluation of the metal layer resistance, or to improve the substrate wetting ability at subsequent annealing and shape improvement of particles and optimization of their sizes. Naturally, the SiO<sub>2</sub> layer additionally contributes to the resulting response, and it is necessary to take into account its thickness and dispersion of optical constants when analyzing optical properties.

On initial *p*-type Si plates with acceptor impurity concentration  $N_B \sim 1 \cdot 10^{16} \text{ cm}^{-3}$ , by chemical deposition from solution of 0.02M AgNO<sub>3</sub> in 5MHF with a component ratio of 1:1 and a deposition time of 30 s, an island film of silver nanoparticles [12] was formed. The chemical method for obtaining Ag nanoparticle layer does not require the creation of SiO<sub>2</sub> layer on silicon and does not create it after nanoparticle deposition. Thus, when determining  $\varepsilon$ , this layer was not included in the analysis of experimental data, since the thickness of the natural SiO<sub>2</sub> layer, measured with an ellipsometer, was only 1 nm and not influenced other parameters of the model.

## 3. Study of the optical properties of the Ag nanoparticle layer

### 3.1. Measurement of spectra

The measurements were carried out using a SE2000 spectral ellipsometer (Semilab Semiconductor Physics Laboratory Co, Ltd. Budapest, Hungary) according to the scheme of an ellipsometer with a rotating compensator and according to the scheme of a stoke-ellipsometer. When using the device as an ellipsometer, two spectra were simultaneously determined in the form of a parameter  $\psi$  (the ratio of complex reflection coefficients  $r_p/r_s$ ) and a parameter  $\Delta$  (phase shift between  $r_p$  and  $r_s$ ), where the index *p* corresponds to the case when the electric vector is parallel to the incidence plane, and the index *s* – to the case when the electric vector is perpendicular to the incidence plane. The parameters  $\psi$  and  $\Delta$  are related to  $r_p$  and  $r_s$ , as well as to the incidence angle  $\varphi$  with respect to the normal to the sample surface in the fundamental equation of ellipsometry [10]:

$$\rho = r_p/r_s = \tan \psi e^{i\Delta}. \quad (1)$$

The polarization reflection spectra  $R_p$  and  $R_s$  were determined using the stoke-ellipsometer scheme. In these measurements, a thick Al layer on a Si plate was used as

a reference mirror. In both schemes, the angle  $\varphi = 70^\circ$  was used in the wavelength range from UV to near IR:  $\lambda = 200\text{--}1700 \text{ nm}$  (0.73–6.2 eV). The use of spectral ellipsometry and spectrophotometry with one instrument provides two advantages: firstly, the ability to measure at the same point of the sample, and secondly, the angle  $\varphi$  is the same for both ellipsometric and spectrophotometric measurements, which is convenient and minimizes errors in pointing of the probing beam (diameter of its spot on the sample  $\sim 400 \mu\text{m}$ ).

### 3.2. Calculation part

#### 3.2.1. Definition of the pseudodielectric function $\langle \varepsilon \rangle$

The term „pseudodielectric function“ is usually used in ellipsometry to analyze the combined response from the bulk material of the substrate and some contribution from the surface layer, taking into account the light penetration depth of tens of nanometers [13]. The calculation of the complex pseudodielectric function  $\langle \varepsilon \rangle$  for a thin film on a substrate was carried out using a simple „substrate-medium“ model based on the measured  $\psi$  and  $\Delta$  with calculation  $\rho$  according to (1) and further calculation according to the formula

$$\begin{aligned} \langle \varepsilon \rangle &= \langle \varepsilon_1 \rangle + i \langle \varepsilon_2 \rangle \\ &= \sin^2(\varphi) \{ 1 + [(1 - \rho)^2 / (1 + \rho)^2] \tan^2(\varphi) \}, \quad (2) \end{aligned}$$

where  $\langle \varepsilon_1 \rangle$  and  $\langle \varepsilon_2 \rangle$  — the real and imaginary parts of  $\langle \varepsilon \rangle$ .

#### 3.2.2. Determination of the dielectric function $\varepsilon$ and film thickness

When using two measurement methods ( $\psi, \Delta$ ) and  $R$  to determine the dielectric function  $\varepsilon$  (real  $\varepsilon_1$  and imaginary  $\varepsilon_2$  parts) of the layer, it is necessary to select a model that describes its parameters and search for them until the calculated and experimental data converge well. In this case, ellipsometry has an advantage over spectrophotometry, since the search and determination of the model parameters occur using two experimental dependences ( $\psi, \Delta$ ), while in the second case — only one dependence  $R$ .

Conduction electrons in noble metals are unbound, their response to an incident electromagnetic wave in the form of a complex dielectric function  $\varepsilon(\omega)$  is described by the Drude formula [7]:

$$\varepsilon(\omega) = \varepsilon_\infty - \omega_p^2 / (\omega^2 + i\Gamma\omega), \quad (3)$$

where  $\omega$  — frequency,  $\varepsilon_\infty$  — dielectric function at infinite frequency,  $\omega_p$  — plasma frequency,  $\Gamma$  — attenuation. Accuracy of this model decreases as we approach the energy of Ag interband transitions, where bound electrons contribute to the dielectric function in the UV region, and the lowest interband transition is at  $\hbar\omega = 3.8 \text{ eV}$ , corresponding to the  $4d\text{--}5s$ . Interband transitions and other

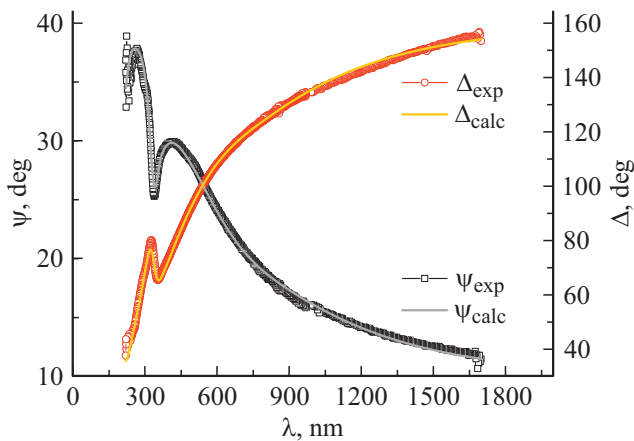


**Figure 1.** Measured dependences  $(\psi, \Delta)_{\text{exp}}$  (symbols) and obtained by fitting according to the D-L model  $(\psi, \Delta)_{\text{calc}}$  (solid lines) for Ag nanoparticle layer on a Si surface for an incidence angle of  $70^\circ$ .

oscillators can be modeled as the contribution of several Lorentzian oscillators:

$$\epsilon(\omega) = \epsilon_\infty + \sum_{j=0}^n f_j / (\omega_j^2 - \omega^2 + i\Gamma\omega), \quad (4)$$

where  $f_j$  – the oscillator amplitude,  $\omega_j$  – the value of plasma frequency,  $n$  – the number of oscillators.

For a film with a certain thickness  $d$ , using the Drude-Lorentz formulas (3) and (4) the dependence  $\epsilon$  was calculated, the  $r_p$  and  $r_s$  and ellipsometric angles  $(\psi, \Delta)_{\text{calc}}$ , which were compared with the measured ones  $(\psi, \Delta)_{\text{exp}}$ , were calculated. By varying the model parameters and thickness, a regression analysis was carried out with minimization of the quality function and fixation of the found model parameters, effective layer thickness  $d_{\text{ef}}$ , and spectral dependence  $\epsilon$ .

A similar approach in solving the inverse problem described above was used to fit the calculated spectra  $(R_p, R_s)_{\text{calc}}$  to the experimental ones  $(R_p, R_s)_{\text{exp}}$  with definition of  $\epsilon$ .

#### 4. Determination of $\langle \epsilon \rangle$ and $\epsilon$ based on ellipsometric angles $(\psi, \Delta)$

Figure 1 shows the measured ellipsometric angles  $(\psi, \Delta)_{\text{exp}}$  for Ag nanoparticle layer on the Si surface for  $\varphi = 70^\circ$ . These data were used to directly calculate  $\langle \epsilon \rangle$  (Fig. 2) and determine  $\epsilon$  using the D-L model (Fig. 3) using the ellipsometer software (SEA (WinElli 3) Ver.1.7.1).

Figure 2 shows the  $\langle \epsilon \rangle$  functions in the form of real  $\langle \epsilon_1 \rangle$  and imaginary  $\langle \epsilon_2 \rangle$  parts calculated with using (1) for experimental  $(\psi, \Delta)_{\text{exp}}$  (Fig. 1). Graphs of  $\langle \epsilon \rangle$  are shown depending on wavelength  $\lambda$  (Fig. 2, a) and photon energy  $E$  (Fig. 2, b). The magnitude  $\langle \epsilon_1 \rangle$  in Fig. 2, b has negative values only in the region  $\lambda = 200\text{--}600$  nm (2.1–5 eV) and

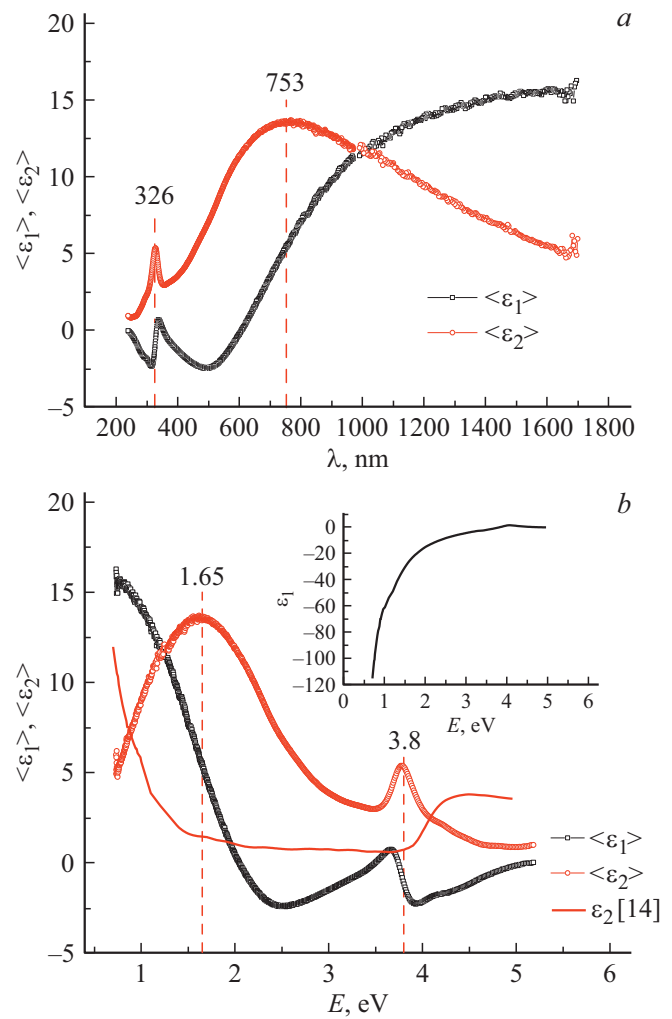


**Figure 2.** Pseudodielectric functions  $\langle \epsilon_1 \rangle$  and  $\langle \epsilon_2 \rangle$  and positions of maxima of functions  $\langle \epsilon_2 \rangle$  volume (326 nm) and localized (753 nm) plasmon resonances of the Ag layer on the Si substrate depending on the wavelength  $\lambda$  (a) and the energy  $E$  (b) at an incidence angle  $\varphi = 70^\circ$ . Dependences  $\epsilon_2$  for bulk Ag [14] in Fig. 2, b,  $\epsilon_1$  — in insertion.

this differs significantly from the case of a continuous film of bulk Ag [14], for which it is negative in almost the entire range (insertion in Fig. 2, b). In our earlier study of Ag nanoparticle layers on Si [15], the dependence  $\langle \epsilon_2 \rangle$  at small thicknesses up to 50 nm reveals the optical features of the substrate (s-Si) in the UV region of the spectrum [16]. In Fig. 2 these features of s-Si in  $\langle \epsilon_2 \rangle$  did not appear in any way.

In the function  $\langle \epsilon_2 \rangle$ , two features are observed in the form of a characteristic peak at  $\lambda = 326$  nm ( $E = 3.8$  eV), as well as a wide symmetric rise  $\langle \epsilon_2 \rangle$  with a maximum at 1.65 eV (753 nm). The peak observed in  $\langle \epsilon_2 \rangle$  at  $E = 3.8$  eV is attributed to volume plasmon resonance in the longitudinal mode [2]. Determination of  $\langle \epsilon \rangle$ , unfortunately, does not allow for revealing thickness of the studied film and its dielectric function, and therefore has limited application.

Optical parameters of Ag nanoparticle layer obtained from ellipsometry using the Drude-Lorentz model

$\varepsilon_\infty$	Drude		Lorentz oscillator 1		Lorentz oscillator 2			
	$\hbar\omega_p$ , eV	$\hbar\Gamma$ , eV	$\hbar\omega_1$ , eV	$f$	$\hbar\Gamma$ , eV	$\hbar\omega_2$ , eV	$f$	$\hbar\Gamma$ , eV
1.95	1.0	0.69	3.79	0.43	0.57	1.99	8.59	1.60

The use of the D-L model makes it possible to determine both  $\varepsilon$  and the film thickness. Analyzing the dependences of  $\langle\varepsilon_2\rangle$  in Fig. 2, one can single out two regions where its growth manifests itself: in the region with a maximum at  $\lambda = 753$  nm, as well as a distinct peak at  $\lambda = 326$  nm. Using their location, further parameters of two Lorentz oscillators (4) and two Drude parameters (3) were introduced into the D-L model. Taking into account that the nanoparticle layer does not have a smooth (parallel) interface between the particles and the medium (air), it is correct to use the term „effective thickness“ and the designation  $d_{ef}$ , which will be applied further. Thus, by introducing another unknown parameter  $d_{ef}$ , all model parameters were fitted by achieving the best convergence between the calculated and experimental ones ( $\psi, \Delta$ ). The D-L parameters determined by this model are presented in the table, and the layer thickness  $d_{ef}$  was  $56 \pm 1$  nm. The resulting dielectric functions  $\varepsilon_1$  and  $\varepsilon_2$  of Ag nanoparticle layer are shown in Fig. 3.

Dependencies  $\langle\varepsilon\rangle$  in Fig. 2 are also added there for comparison. The dependences  $\varepsilon_1$  and  $\langle\varepsilon_1\rangle$  are close in the UV and visible regions, while there is a difference in the near-IR region. The difference is more clearly seen when comparing  $\varepsilon_2$  with  $\langle\varepsilon_2\rangle$  in the  $\lambda = 670$ – $1700$  nm region. The film becomes less absorbent, as can be seen from the lower location of the function  $\varepsilon_2$  derived from

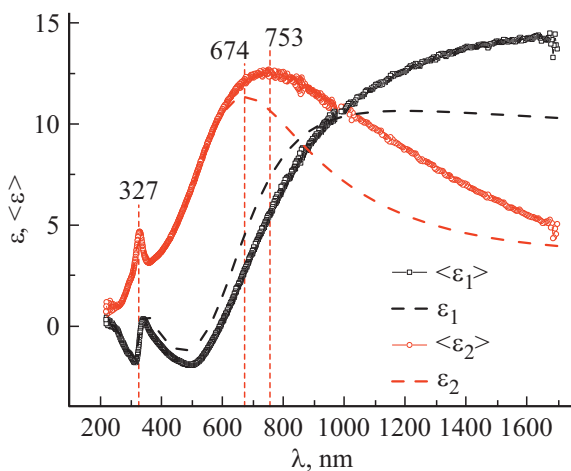


**Figure 3.** Comparison of pseudodielectric functions  $\langle\varepsilon_1\rangle$  and  $\langle\varepsilon_2\rangle$  (solid lines) and dielectric functions  $\varepsilon_1$  and  $\varepsilon_2$  (dashed lines) obtained by fitting the calculated spectra  $(\psi, \Delta)_{calc}$  according to the D-L model to the experimental ones  $(\psi, \Delta)_{exp}$  for Ag layer on Si substrate.

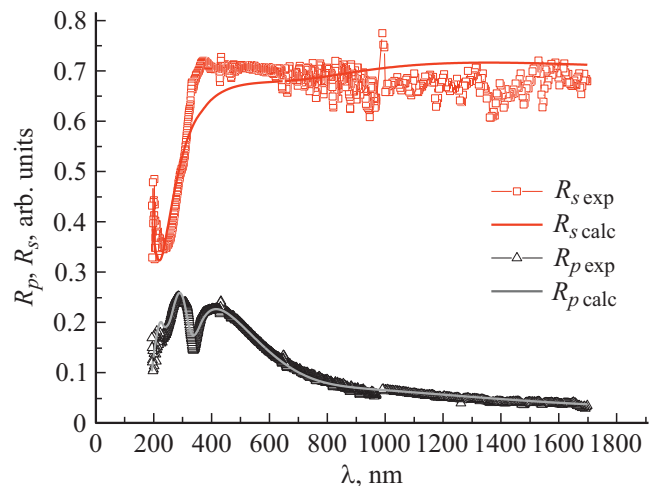


**Figure 4.** Experimental reflection spectra for  $p$ - and  $s$ -polarizations  $R_{p,exp}$  and  $R_{s,exp}$  (symbols) and calculated ones  $R_{p,calc}$  and  $R_{s,calc}$  (solid lines) obtained using the D-L model for Ag nanoparticle layer on a Si surface at an incidence angle of  $70^\circ$ .

the D-L equation compared to the function  $\langle\varepsilon_2\rangle$ . It follows that the higher location of  $\langle\varepsilon_2\rangle$  is the result „of addition“ of absorption from the Si substrate. Almost complete coincidence of the dependences  $\varepsilon_2$  and  $\langle\varepsilon_2\rangle$  is noted in the volume plasmon resonance region (3.8 eV), where collective oscillations of bound and free electrons occur. This indicates the possibility to determine  $\langle\varepsilon\rangle$  along with  $\varepsilon$  for a layer of Ag nanoparticles on a Si substrate, but without determining film thickness.

The rise of  $\varepsilon_2$  with a maximum at  $\lambda_{max} = 674$  nm is a manifestation of localized plasmon resonance. This maximum does not coincide with the position of the maximum in  $\langle\varepsilon_2\rangle$  ( $\lambda_{max} = 753$  nm), since in this range the optical properties of the substrate already affect the total optical response. Nevertheless, the use of a quick determination of  $\langle\varepsilon\rangle$  is useful for establishing the resonance position on the spectrum, which facilitates the subsequent determination of  $\varepsilon$  already using the regression analysis method.

## 5. Determination of $\varepsilon$ from polarization spectra $R_p$ and $R_s$

Determination  $\varepsilon$  of a nanoparticle layers was carried out by measuring  $R_p$  and  $R_s$ . The same procedure was applied using the D-L model, entering its parameters and the expected layer thickness to calculate the initial  $\varepsilon$  and its subsequent search. It was assumed that the desired layer thickness  $d_{ef}$  would be the same for  $p$ - and  $s$ -polarizations. Further, the obtained  $\varepsilon$  was used to calculate  $R$ , compared with  $R_{exp}$  until the maximum convergence was obtained, as was done above with ellipsometric angles ( $\psi, \Delta$ ).

The measured spectra  $R_{p,exp}$  and  $R_{s,exp}$  are shown in Fig. 4, which shows that the spectrum  $R_{s,exp}$  is quite noisy in

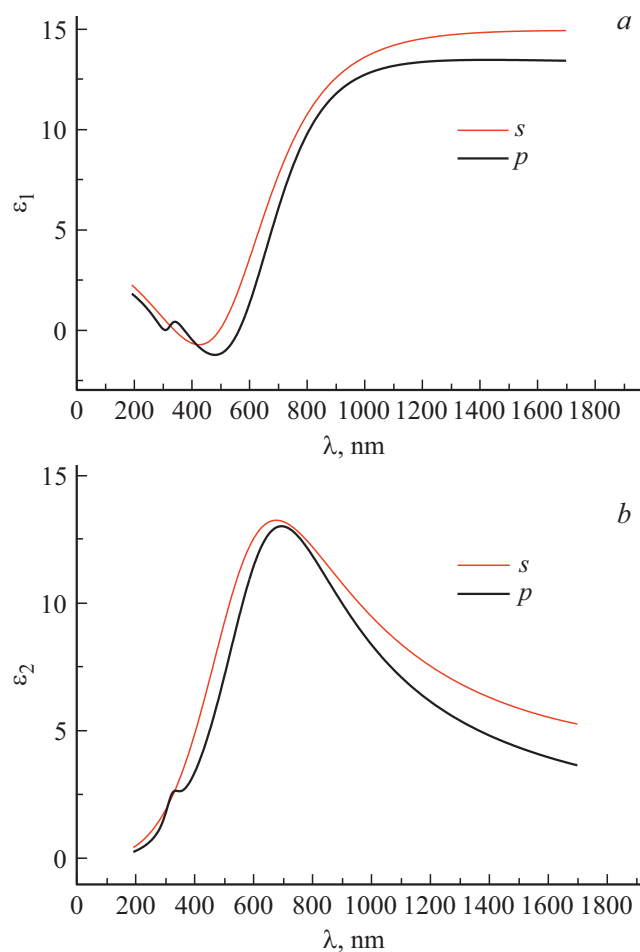


**Figure 5.** Dielectric functions  $\varepsilon_1$  and  $\varepsilon_2$  for  $p$ - and  $s$ -polarizations determined by the D-L model for Ag nanoparticle layer as a result of analysis of spectra  $R_p$  and  $R_s$ . Layer thickness  $d_{ef} = 54 \pm 1$  nm.

the range  $\lambda = 600\text{--}1700$  nm. Since the nanoparticle layer is not continuous, the presence of noise from random light scattering from particles was expected. At the same time, the spectrum of  $R_{p\text{exp}}$  turned out to be without significant fluctuations. The calculated spectra  $R_{p\text{calc}}$  and  $R_{s\text{calc}}$  are also shown, obtained by varying the parameters of the D-L model and the layer thickness, and which maximally coincide with the experimental spectra  $R_{p\text{exp}}$  and  $R_{s\text{exp}}$  as a result of fitting.

The dependences  $\varepsilon_1$  and  $\varepsilon_2$ , extracted by fitting to experimental ones  $R_p$  and  $R_s$  using the D-L formula, are shown in Fig. 5 for the established Ag nanoparticle layer thickness  $d_{ef} = 54 \pm 1$  nm. This value, within the error, agrees well with the film thickness determined by spectral ellipsometry ( $d_{ef} = 56$  nm).

The values  $\varepsilon$  differ for  $p$ - and  $s$ -polarizations, but only slightly. As expected from the ellipsometric results presented above, the dependences  $\varepsilon_1$  and  $\varepsilon_2$  with  $p$ -polarization exhibit a volume plasmon peak at  $E = 3.8$  eV, which has already been discussed in this article, and also

manifested itself in the spectra  $R_p$  for island films in the article [15].

## Conclusions

Ag nanoparticle layer deposited on a single-crystal Si substrate from an  $\text{AgNO}_3$  solution is characterized by spectral ellipsometry and reflective spectrophotometry on the same device.

To interpret the measured ellipsometric data, two models were used: „external medium-substrate“ model with definition of the pseudodielectric function and the „external medium-film-substrate“ model using the D-L formula. This allowed us to determine both the complex dielectric function and the island film effective. Also, within the framework of the D-L model, spectrophotometric data were processed with determination of dielectric functions similar in shape for the  $p$ - and  $s$ -polarizations of the incident light, assuming the same thickness  $d_{ef}$  of Ag- layers.

Dielectric functions are studied in a wide spectral range from UV to near-IR with optical and resonant features. Complete coincidence of the dependences  $\varepsilon_2$  and  $\langle\varepsilon_2\rangle$  is observed in the volume plasmon resonance region (3.8 eV), where collective oscillations of bound and free electrons occur. Using spectral ellipsometry and spectrophotometry, this plasmon at  $\lambda = 326$  nm ( $E = 3.8$  eV) in the function  $\varepsilon_2$  is well determined using both methods. Differences between the  $\varepsilon$  and  $\langle\varepsilon_2\rangle$  dependences, as well as in the spectral position of the localized plasmon resonance, are identified.

## Funding

The work was carried out using state budget funds on the topic of state assignment 0040-2019-0012.

## Conflict of interest

The authors declare that they have no conflict of interest.

## References

- [1] S.A. Maier. *Plasmonics: Fundamentals and Applications* (Springer Science+Business Media LLC, NY, 2007).
- [2] M.I. Stockman. *Science*, **348** (6232), 287 (2015). DOI: 10.1126/science.aaa6805
- [3] H.A. Atwater, A. Polman. *Nature Materials*, **9** (3), 205 (2010). DOI: 10.1038/nmat2629
- [4] V.M. Shalaev. *Nat. Photonics*, **1**(1), 41 (2007). DOI: 10.1038/nphoton.2006.49
- [5] Y. Wang, E.W. Plummer, K. Kempa. *Adv. Phys.*, **60** (5), 799 (2011). DOI: org/10.1080/00018732.2011.621320
- [6] M.I. Stockman, K. Kneipp, S.I. Bozhevolnyi et al. *J. Opt.*, **20** (4), 043001 (2018). DOI: org/10.1088/2040-8986/aaa114
- [7] T.W.H. Oates, H. Wormeester, H. Arwin. *Progr. Surf. Sci.*, **86** (11–12), 328 (2011). DOI: org/10.1016/j.progsurf.2011.08.004

- [8] A. Hilgerm, M. Tenfeldeu, U. Kreibig. *Appl. Phys. B.*, **73** (4), 361 (2001). DOI: 10.1007/s003400100712
- [9] V.A. Kosobukin. *Phys. Sol. St.*, **54** (12), 2471 (2012).
- [10] R.M.A. Azzam, N.M. Bashara. *Ellipsometry and Polarized Light* (North-Holland Publ. Co., Amsterdam-NY-Oxford, 1977) (M.: Mir, 1981).] (in Russian).
- [11] H. Fujiwara. *Spectroscopic Ellipsometry. Principles and Applications* (Wiley John & Sons Ltd., England, 2007).
- [12] Yu.A. Zharova, V.A. Tolmachev, A.I. Bednaya, S.I. Pavlov. *Semicond.*, **52** (3), 316 (2018).  
DOI: org/10.1134/S1063782618030235
- [13] H.U. Yang, J. D'Archangel, M.L. Sundheimer, E. Tucker, G.D. Boreman, M.B. Raschke. *Phys. Rev. B.*, **91** (23), 235137 (2015). DOI: org/10.1103/PhysRevB.91.235137
- [14] *Handbook of Optical Constants of Solids*. Ed. by E.D. Palik (Academic Press, NY., 1985).
- [15] V.A. Tolmachev, Yu.A. Zharova, S.A. Grudinkin. *Opt. i spektr.*, **128** (12), 1868 (2020) (in Russian).  
DOI: 10.21883/OS.2020.12.50324.211-20;  
V.A. Tolmachev, Yu.A. Zharova, S.A. Grudinkin. *Optics and Spectroscopy*, **128** (12), 2002 (2020).  
<https://doi.org/10.1134/S0030400X20121066>
- [16] D.E. Aspnes. *Thin Solid Films*, **89** (3), 249 (1982).  
DOI: org/10.1016/0040-6090(82)90590-9